ERICE PREPRINT SERIES

«ETTORE MAJORANA» CENTRE FOR SCIENTIFIC CULTURE



EMCSC/ELN 93–02
19 March 1993

# MULTI-JET RATES IN DEEP INELASTIC SCATTERING AND IN $e^+e^-$ ANNIHILATION

G. Anzivino, F. Arzarello, G. Bari, M. Basile, E. Blanco, L. Bellagamba, D. Boscherini, G. Bruni, P. Bruni, G. Cara Romeo, M. Chiarini, L. Cifarelli, F. Cindolo, F. Ciralli, A. Contin, S. D'Auria, C. Del Papa, S. De Pasquale, F. Fiori, F. Frasconi, P. Giusti, G. Iacobucci, G. Maccarrone, A. Margotti, T. Massam, R. Nania, F. Palmonari, S. Qian, G. Sartorelli, M. Schioppa, Yu. M. Shabelski, G. Susinno, R. Timellini, L. Votano and A. Zichichi

CERN, Geneva, Switzerland
INFN, Bologna, Italy
INFN, Eloisatron Project, Erice, Italy
INFN, LNF, Frascati, Italy
Physics Department, University of Bologna, Italy
Physics Department, University of Calabria, Cosenza, Italy
Physics Department, University of Pisa, Italy
PNPI, Gatchina, St. Petersburg, Russia
World Laboratory, Lausanne, Switzerland

## Abstract

Predictions for multi-jet rates in deep inelastic scattering (DIS), in the current fragmentation region, and in $e^+e^-$ annihilation are derived using the so-called "$k_\perp$-clustering" algorithm. The dependence of these rates vs. $Q^2$ and $y_{cut}$ (the jet resolution parameter) is studied in detail and presented as an interesting test of perturbative QCD approaches for HERA and LEP (I and II) experiments.

*(Submitted to Il Nuovo Cimento)*

## 1. INTRODUCTION

The comparison of experimental data on multi-jet rates with QCD calculations gives the possibility to test the existing (leading-order as well as next-to-leading order) perturbative approaches and to measure the strong coupling $\alpha_s$, one of today's most crucial quantities, with better accuracy (see [1]). Theoretical formulae exist for gluon and quark jets whereas experimentally hadron jets are observed. Therefore this comparison would also allow to gain information on parton-hadron transition mechanisms.

As analysed in detail in [2], the theoretical accuracy of jet production probabilities depends significantly on the algorithm adopted for jet identification. In [3] a new algorithm was proposed for $e^+e^-$ collisions, the so-called "$k_\perp$-clustering" algorithm [3] or "Durham" algorithm [2], which allows one to determine if two particles, $i$ and $j$, belong to the same jet or not. In accordance with [3] one should calculate the quantity:

$$y_{ij} = \frac{2(1-\cos\Theta_{ij}) \cdot \min(E_i^2, E_j^2)}{Q^2}, \tag{1}$$

where $E_i$, $E_j$ are the particle energies and $\Theta_{ij}$ their angular aperture. Particles $i$ and $j$ belong to one jet only if their relative, scaled transverse momentum $y_{ij}$ is smaller than the value of a special parameter $y_{cut} = Q_0^2/Q^2 < 1$, the so-called "resolution parameter". If it is so, this jet is considered as a new "pseudoparticle". Then the procedure is repeated for pseudoparticle $ij$ (with four-momentum $p_{ij} = p_i + p_j$) and a third particle $k$, and so on. Of course, the energies of the particles considered should not be too small, i.e. $E_i, E_j, E_k \gg \Lambda_{QCD}$. It was shown in [2, 4] that algorithm (1) has better theoretical properties than the JADE algorithm [5] which is the most commonly used method for defining and reconstructing jets via a different, invariant mass-type variable:

$$y_{ij} = \frac{2(1-\cos\Theta_{ij}) \cdot E_i \cdot E_j}{Q^2}. \tag{2}$$

Recently, a modified version of the $k_\perp$-clustering algorithm has been proposed for the deep inelastic scattering (DIS) case [6], in particular to identify jets in the current fragmentation (CF) region. In the present work we will use this algorithm for QCD calculations of multi-jet production probabilities in deep inelastic scattering and $e^+e^-$ annihilation, keeping in mind the ongoing and future experiments at HERA and LEP-I, LEP-II.

## 2. JET DEFINITION AND JET COUNTING

In $e^+e^-$ annihilation the multi-jet production probabilities for 2 jets (i.e. two quark jets), 3 jets (i.e. two quark and one gluon jets) and 4 jets (i.e. two quark and two gluon jets) in the next-to-leading order QCD approach are [3]:

$$R_2^{e^+e^-} = [\Delta_q(Q)]^2, \tag{3}$$

$$R_3^{e^+e^-} = 2[\Delta_q(Q)]^2 \int_{Q_0}^{Q} dq \Gamma_q(Q,q)\Delta_g(q), \tag{4}$$

$$R_4^{e^+e^-} = 2[\Delta_q(Q)]^2[(\int_{Q_0}^{Q} dq\Gamma_q(Q,q)\Delta_g(q))^2 + \int_{Q_0}^{Q} dq\Gamma_q(Q,q)\Delta_g(q)\int_{Q_0}^{q} dq'\Gamma_g(q,q')\Delta_g(q') + \int_{Q_0}^{Q} dq\Gamma_q(Q,q)\Delta_g(q)\int_{Q_0}^{q} dq'\Gamma_f(q')\Delta_f(q')], \quad (5)$$

where $Q \sim \sqrt{s}$ is the scale of the jet production process, $Q_0 = \sqrt{y_{cut}} \cdot Q$, $\Delta_q(Q)$ and $\Delta_g(Q)$ are the quark and gluon Sudakov form factors, and $\Gamma_q(Q,q)$ and $\Gamma_g(Q,q)$ the parton splitting probabilities. These quantities have the following expressions:

$$\Delta_q(Q) = \exp(-\int_{Q_0}^{Q} dq\Gamma_q(Q,q)), \quad (6)$$

$$\Delta_g(Q) = \exp(-\int_{Q_0}^{Q} dq[\Gamma_g(Q,q) + \Gamma_f(q)]), \quad (7)$$

$$\Delta_f(q) = [\Delta_q(q)]^2/\Delta_g(q), \quad (8)$$

$$\Gamma_q(Q,q) = \frac{2C_F}{\pi}\frac{\alpha_s(q)}{q}(\ln\frac{Q}{q} - \frac{3}{4}), \quad (9)$$

$$\Gamma_g(Q,q) = \frac{2C_A}{\pi}\frac{\alpha_s(q)}{q}(\ln\frac{Q}{q} - \frac{11}{12}), \quad (10)$$

$$\Gamma_f(q) = \frac{N_f}{3\pi}\frac{\alpha_s(q)}{q}, \quad (11)$$

where $N_f = 5$ is the number of flavours and $C_F = (N_c^2 - 1)/2N_c = 4/3$ and $C_A = N_c = 3$ are the colour factors. We use the leading-order expression for $\alpha_s$:

$$\alpha_s(q) = \frac{12\pi}{(33 - 2N_f)\ln q^2/\Lambda^2}. \quad (12)$$

The formulae given in [3] for the above $n$-jet fractions $R_n^{e^+e^-}$ (eqs. (3)-(5)) hold true for small values of $y_{cut}$, i.e. $y_{cut} \ll 1$, and use the fact that in the perturbative expansions in $\alpha_s$, the large logarithmic terms of the form $\alpha_s^i \ln^j y_{cut}$ (with $i < j \leq 2i$) exponentiate and therefore resummation of leading and next-to-leading order logarithms is achieved to all order in $\alpha_s$. However, if $y_{cut}$ is not small enough, eqs. (9) and (10) produce negative values of $\Gamma_q(Q,q)$ and $\Gamma_g(Q,q)$ which in turn can produce Sudakov form factors larger than unity and/or negative $n$-jet probabilities. To avoid such a problem, we will restrict ourselves to the range $y_{cut} = 10^{-4} \div 10^{-2}$ and use only positive values of $\Gamma_q(Q,q)$, $\Gamma_g(Q,q)$ and $\Gamma_g(Q,q)+\Gamma_f(q)$, setting them equal to zero when negative (i.e. changing $\Gamma = \Gamma_q, \Gamma_g$ or $\Gamma_g+\Gamma_f$ with $\Gamma\cdot\Theta(\Gamma)$, where $\Theta(\Gamma) = 0$ if $\Gamma < 0$ and $\Theta(\Gamma) = 1$ if $\Gamma > 0$). Of course, since $y_{cut}$ is small enough, all results with or and without such restriction are practically the same as we will see in sect. 3.

Turning now to the DIS case, the QCD formulae needed to derive $n$-jet production probabilities in the current fragmentation region at the next-to-leading order were obtained from [6]. In the Breit frame of the incoming hadron and the exchanged vector particle (where the latter has zero energy and momentum opposite to the incoming hadron momentum), the $k_\perp$-clustering algorithm is applied in two steps to define: a "beam jet" (containing the proton

remnants) relative to the target fragmentation (TF) region and a number of "macro-jets" relative the current fragmentation (CF) region. Beam jet and macro-jets are identified using a hard scattering resolution scale $E_t$, with $Q^2 \geq E_t^2 \gg \Lambda_{QCD}$, i.e. using the quantity $y_{ij}$ given by eq. (1) with $E_t^2$ (instead of $Q^2$) in the denominator and $y_{cut} = 1$. In the CF region, macro-jets are then resolved into single jets using again the variable $y_{ij}$ as for macro-jets, but with a finer resolution parameter $y_{cut} = Q_0^2/E_t^2 < 1$. What is special about the Breit frame is that multi-jet probabilities, as derived via the $k_\perp$-clustering algorithm [6] in CF, turn out to be independent of both $x$ and $y$, the standard kinematic quantities of DIS[1]. Notice that in this frame $Q$ is the absolute value of the exchanged vector particle momentum (with $Q = 2xP$, where $P$ is the absolute value of the initial hadron momentum). We will consider the simplest case when $E_t^2 = Q^2$, which implies [6] that only the struck quark is responsible for jet production in the CF region. In [6] formulae are given for the exclusive $n$-jet structure functions $F^n(x, Q^2, y_{cut})$ which are proportional to the usual inclusive structure function $F_2(x, Q^2)$. The ratios $F^n(x, Q^2, y_{cut})/F_2(x, Q^2)$ have the meaning of probabilities ($R_n^{DIS}$) of $n$-jet production in the current fragmentation region. These probabilities for 1 jet (i.e. only one quark jet), 2 jets (i.e. one quark and one gluon jets) and 3 jets (i.e. one quark and two gluon jets) in the CF region of DIS have the following expressions [6]:

$$R_1^{DIS} = \Delta_q(Q), \tag{13}$$

$$R_2^{DIS} = \Delta_q(Q) \int_{Q_0}^{Q} dq \Gamma_q(Q, q) \Delta_g(q), \tag{14}$$

$$\begin{aligned} R_3^{DIS} \;=\; & \Delta_q(Q)[\frac{1}{2}(\int_{Q_0}^{Q} dq \Gamma_q(Q, q) \Delta_g(q))^2 \\ & + \int_{Q_0}^{Q} dq \Gamma_q(Q, q) \Delta_g(q) \int_{Q_0}^{q} dq' \Gamma_g(q, q') \Delta_g(q') \\ & + \int_{Q_0}^{Q} dq \Gamma_q(Q, q) \Delta_g(q) \int_{Q_0}^{q} dq' \Gamma_f(q') \Delta_f(q')], \end{aligned} \tag{15}$$

with the same definitions as in eqs. (3)-(5). Let us emphasize once more that all these probabilities do not depend on $x$. This implies that the corresponding structure functions $F^n(x, Q^2, y_{cut})$ have the same $x$ dependence as $F_2(x, Q^2)$. Here again we have the problem of negative values for $\Gamma_q(Q, q)$ and $\Gamma_g(Q, q)$ and we will solve it in the same way as for $e^+e^-$ annihilation.

For details concerning this section, we refer the reader to [2-4, 6]. As a final remark, let us point out that in the Breit reference system, the CF region of DIS closely reminds the $e^+e^-$ final state: there is one outgoing quark with energy $Q/2$ instead of two [7].

## 3. JET RATES IN DEEP INELASTIC SCATTERING AND $e^+e^-$ ANNIHILATION

The calculated probabilities $R_n^{DIS}$ of 1, 2 and 3-jet production in the CF region of DIS at $Q^2 = 10^3$ GeV$^2$ are presented in fig. 1 vs. $y_{cut}$: the solid curves correspond to only positive values of $\Gamma_q(Q, q)$, $\Gamma_g(Q, q)$ and $\Gamma_g(Q, q) + \Gamma_f(q)$ (i.e. with $\Theta$-function) and the dashed ones

1) This does not happen using JADE-type algorithms for jet finding.

to the values obtained with eqs. (9) and (10). The differences between the solid and dashed curves are not large and decrease at very small values of $y_{cut}$, as expected. The value of $\Lambda$ in eq. (12) is 0.2 GeV. Notice that here and in the following the values of $Q^2$ used in our calculations for DIS are chosen to match the HERA range.

There is some uncertainty in the choice of the $\Lambda$ value to be used in our theoretical approach: in fact this $\Lambda$ is not the same as $\Lambda_{\overline{MS}}$ but an effective parameter which should ensure the fastest convergence of the theoretical expansions. For example, in the same framework, previous calculations of the inclusive spectra of secondaries produced in $e^+e^-$ annihilation [8, 9] used $\Lambda = 0.25$ GeV for all charged particles and $\Lambda = 0.15$ GeV for charged pions. To show the dependence of jet production probabilities on $\Lambda$, in fig. 2 these probabilities are plotted vs. $y_{cut}$ for two different values of $\Lambda$, i.e. 0.2 GeV and 0.3 GeV, at $Q^2 = 10^4$ GeV$^2$. The differences are small enough. In the following, unless differently specified, we will adopt the value $\Lambda = 0.2$ GeV in accordance with [10].

With $\Lambda = 0.2$ GeV and $\Theta$-function for $\Gamma_q, \Gamma_g$ and $\Gamma_q+\Gamma_f$, the probabilities $R_n^{DIS}$ for 1, 2 and 3 jets at $Q^2 = 10^3$ GeV$^2$ and $Q^2 = 10^4$ GeV$^2$ are presented in fig. 3 vs. $y_{cut}$ and in fig. 4 vs. $Q^2$ at $y_{cut} = 0.001$ and $y_{cut} = 0.01$. When we go to smaller values of $y_{cut}$ at fixed $Q^2$, the single-jet probability decreases and the multi-jet probabilities increase up to a maximum (whose position, as $Q^2$ increases, moves towards smaller $y_{cut}$ values) and then decrease. This seems to be quite natural because, at very small $y_{cut}$, any particle with sufficient energy will be considered as a separate jet. These multi-jet probabilities slightly decrease with increasing $Q^2$ at fixed values of $y_{cut}$ (fig. 4), while $R_1^{DIS}$ increases. At $y_{cut} = 0.01$, there is a gap between the single-jet and multi-jet probabilities, $R_1^{DIS}$ being in fact significantly higher (fig. 4). This gap disappears as $y_{cut}$ goes down to 0.001 as a consequence of what already observed in fig. 3, i.e. the lower is $y_{cut}$, the higher is the multiplicity of identified jets. Finally let us note that if we fix the value of $\alpha_s$, the jet production probabilities become $Q^2$-independent.

For $e^+e^-$ annihilation the probabilities $R_n^{e^+e^-}$ of 2, 3 and 4-jet production at LEP-I energy ($Q^2 = 8 \cdot 10^3$ GeV$^2$), are presented in fig. 5 as functions of $y_{cut}$. As in fig. 1, the solid curves, corresponding to only positive values of $\Gamma_q(Q,q)$, $\Gamma_g(Q,q)$ and $\Gamma_q(Q,q)+\Gamma_g(Q,q)$, and the dashed ones, corresponding to the values obtained with eqs. (9) and (10), are very close.

The dependence of the $R_n^{e^+e^-}$ probabilities on $\Lambda$ is also small as it appears in fig. 6 where these are shown at LEP-II energy ($Q^2 = 4 \cdot 10^4$ GeV$^2$), as functions of $y_{cut}$ for $\Lambda = 0.2$ GeV and $\Lambda = 0.3$ GeV.

With the same options as in DIS for $\Gamma_q$, $\Gamma_g$, $\Gamma_g+\Gamma_f$ and $\Lambda$, the $R_n^{e^+e^-}$ probabilities of 2, 3 and 4 jets in $e^+e^-$ annihilation as functions of $y_{cut}$ (at fixed $Q^2$) and of $Q^2$ (at fixed $y_{cut}$) are presented in figs. 7 and 8, respectively. In both figures, the qualitative behaviour of the curves is similar to the DIS case (figs. 3 and 4). We can see in fig. 7 that $R_2^{e^+e^-}$ (which closely reminds $R_1^{DIS}$ in fig. 3, i.e. the minimal jet-configuration in the CF region of DIS) decreases as $y_{cut}$ decreases at fixed $Q^2$, while $R_3^{e^+e^-}$ and $R_4^{e^+e^-}$ (like $R_2^{DIS}$ and $R_3^{DIS}$ in fig. 3) increase until they reach a maximum whose position is again $Q^2$-dependent. If we consider $R_n^{e^+e^-}$ vs. $Q^2$ at fixed values of $y_{cut}$ (fig. 8), we can see that at small values of $y_{cut}$ ($y_{cut} = 0.001$) the 2 and 3-jet probabilities increase with $Q^2$ and the 4-jet probability decreases. At a larger value of $y_{cut}$ ($y_{cut} = 0.01$) only the 2-jet probability increases with $Q^2$ and jumps to a much higher level. Again, at fixed values of $\alpha_s$, we obtain jet production probabilities

which do not depend on $Q^2$.

To summarize our results on $e^+e^-$, we present in table 1 the probabilities for 2, 3 and 4 jets corresponding to some typical values of $Q^2$ and $y_{cut}$. The trends are as follows: if we fix the value of the product $y_{cut} \cdot Q^2$ $(= Q_0^2)$, when the energy increases the 2-jet probability decreases and the 4-jet probability increases, while the 3-jet probability shows an intermediate behaviour (increasing at large $y_{cut}$ and decreasing at small $y_{cut}$). If we fix the value of $y_{cut}$, the 2 and 3-jet probabilities increase with increasing energies, but the 4-jet probability decreases.

Finally, the jet production rates in DIS (CF region) and $e^+e^-$ annihilation (full phase-space) are compared in figs. 9 and 10 as functions of $Q^2$ at $y_{cut} = 0.01$ and $y_{cut} = 0.001$, respectively. As already observed (figs. 4 and 8), at fixed $y_{cut}$ $R_n^{DIS}$ and $R_{n+1}^{e^+e^-}$ $(n = 1, 2, 3)$ evolve vs. $Q^2$ in a similar way. However, for each $(R_n^{DIS}, R_{n+1}^{e^+e^-})$ pair of curves in figs. 9 and 10, there is a significant difference in level. In fact, for the same $Q^2$ and $y_{cut}$ values, eqs. (3)-(5) and (13)-(15) simply give:

$$R_2^{e^+e^-} = (R_1^{DIS})^2, \tag{16}$$

$$R_3^{e^+e^-} = 2R_1^{DIS} \cdot R_2^{DIS}, \tag{17}$$

$$R_4^{e^+e^-} = (R_2^{DIS})^2 + 2R_1^{DIS} \cdot R_3^{DIS}. \tag{18}$$

This is of course what expected if the CF region of DIS in the Breit frame should actually correspond to one hemisphere of $e^+e^-$ annihilation. Notice that the CF region of DIS may provide a cleaner environment for accurate jet measurements, due to the absence of combinatorial effects.

## 4. CONCLUSION

In the present work, using the $k_\perp$-clustering algorithm for jet identification, multi-jet rate predictions are derived for deep inelastic scattering (DIS) in the current fragmentation region, in a range of $Q^2$ easily explorable at HERA. Analogous results are obtained for $e^+e^-$ annihilation at LEP-I and LEP-II energies. A detailed study of these rates vs. $Q^2$ and $y_{cut}$ is presented as a guideline for future tests of perturbative QCD. How well these theoretical predictions will be tested experimentally will be crucial to improve our knowledge of the strong coupling $\alpha_s$.

Concerning the DIS case, it would be very interesting if the formulae of [6], giving multi-jet fractions in the current fragmentation region, could be extended also to the target fragmentation region, thus providing a complete picture of jet production in DIS final states. In this case, detailed comparisons of full multi-hadron events in $ep$ and $e^+e^-$ collisions could be achievable. It would be very interesting to check in particular whether the "universality properties" of $ep$, $e^+e^-$ (and, moreover, $pp$ or $\bar{p}p$) interactions, observed at low energy [11], still hold true for the new generation of high-energy machines, namely HERA, LEP-I and II (and Tevatron). In this respect it is worthwhile to recall that the effective energy for hadron

and jet production in a full DIS event, $(Q^2)^{had}_{DIS}$, to be compared with the equivalent energy in $e^+e^-$, $(Q^2)^{had}_{e^+e^-} = (Q^2)_{e^+e^-} = (s)_{e^+e^-}$, is in fact:

$$(Q^2)^{had}_{DIS} = [(q + q^{had})^2]_{DIS} \neq (Q^2)_{DIS} \neq (W^2)_{DIS}$$

where $q = p_1 - p'_1$ ($p_1$ and $p'_1$ being the four-momenta of incoming and outgoing leptons) is the standard four-momentum transfer from the leptonic to the hadronic vertex, $q^{had} = p_2 - p'_2$ ($p_2$ and $p'_2$ being the four-momenta of incoming and outgoing protons) is the effective four-momentum transfer at the hadron vertex once the "leading" proton effect is duly taken into account, and $(Q^2)_{DIS} = -q^2$ and $(W^2)_{DIS} = (p_2 + q)^2$ are the standard DIS variables. Needless to say that full tracking coverage, via the detection of leading protons in very forward region (as foreseen in the ZEUS experiment at HERA [12]), will be crucial to this end.

## ACKNOWLEDGEMENTS

We are grateful to M. Ciafaloni, Yu. L. Dokshitzer, V. A. Khoze and B. R. Webber for stimulating discussions.

## Table 1

Probabilities of 2, 3 and 4-jet production in $e^+e^-$ annihilation.

| $Q^2$ (GeV$^2$) | $y_{cut}$ | $R_2^{e^+e^-}$ | $R_3^{e^+e^-}$ | $R_4^{e^+e^-}$ |
|---|---|---|---|---|
| $10^4$ | 0.01 | 0.683 | 0.253 | 0.060 |
| $10^5$ | 0.001 | 0.341 | 0.342 | 0.206 |
| $10^4$ | 0.001 | 0.240 | 0.312 | 0.243 |
| $10^5$ | 0.0001 | 0.068 | 0.154 | 0.202 |

## Figure captions

Fig. 1 : Probabilities vs. $y_{cut}$ of 1, 2 and 3-jet production in the current fragmentation region of DIS at $Q^2 = 10^3$ GeV$^2$, using for $\Gamma_q$, $\Gamma_g$ and $\Gamma_g + \Gamma_f$ only positive values (solid curves) and the values obtained with eqs. (9) and (10) (dashed curves).

Fig. 2 : Probabilities vs. $y_{cut}$ of 1, 2 and 3-jet production in the current fragmentation region of DIS at $Q^2 = 10^4$ GeV$^2$, for $\Lambda = 0.2$ GeV (solid curves) and $\Lambda = 0.3$ GeV (dashed curves).

Fig. 3 : Probabilities vs. $y_{cut}$ of 1, 2 and 3-jet production in the current fragmentation region of DIS at $Q^2 = 10^4$ GeV$^2$ (solid curves) and $Q^2 = 10^3$ GeV$^2$ (dashed curves).

Fig. 4 : Probabilities vs. $Q^2$ of 1, 2 and 3-jet production in the current fragmentation region of DIS at $y_{cut} = 0.001$ (solid curves) and $y_{cut} = 0.01$ (dashed curves).

Fig. 5 : Probabilities vs. $y_{cut}$ of 2, 3 and 4-jet production in $e^+e^-$ annihilation at $Q^2 = 8 \cdot 10^3$ GeV$^2$, using for $\Gamma_q$, $\Gamma_g$ and $\Gamma_g + \Gamma_f$ only positive values (solid curves) and the values obtained with eqs. (9) and (10) (dashed curves).

Fig. 6 : Probabilities vs. $y_{cut}$ of 2, 3 and 4-jet production in $e^+e^-$ annihilation at $Q^2 = 8 \cdot 10^3$ GeV$^2$, for $\Lambda = 0.2$ GeV (solid curves) and $\Lambda = 0.3$ GeV (dashed curves).

Fig. 7 : Probabilities vs. $y_{cut}$ of 2, 3 and 4-jet production in $e^+e^-$ annihilation at $Q^2 = 8 \cdot 10^3$ GeV$^2$ (solid curves) and $Q^2 = 4 \cdot 10^4$ GeV$^2$ (dashed curves).

Fig. 8 : Probabilities vs. $Q^2$ of 2, 3 and 4-jet production in $e^+e^-$ annihilation at $y_{cut} = 0.001$ (solid curves) and $y_{cut} = 0.01$ (dashed curves).

Fig. 9 : Probabilities vs. $Q^2$ of 1, 2 and 3-jet production in the current fragmentation region of DIS (solid curves) and of 2, 3 and 4-jet production in $e^+e^-$ annihilation (dashed curves) at $y_{cut} = 0.01$.

Fig. 10 : Probabilities vs. $Q^2$ of 1, 2 and 3-jet production in the current fragmentation region of DIS (solid curves) and of 2, 3 and 4-jet production in $e^+e^-$ annihilation (dashed curves) at $y_{cut} = 0.001$.

## REFERENCES


[1] L3 Collaboration (B. Adeva et al.), Phys. Lett. B284 (1992) 471.

[2] S. Bethke, Z. Kunszt, D. E. Soper and W. J. Stirling, Nucl. Phys. B370 (1992) 310.

[3] S. Catani, Yu. L. Dokshitzer, M. Olsson, G. Turnock and B. R. Webber, Phys. Lett. B269 (1991) 432.

[4] S. Catani, B. R. Webber, Yu. L. Dokshitzer and F. Fiorani, Nucl. Phys. B383 (1992) 419.

[5] JADE Collaboration (S. Bethke et al.), Phys. Lett. B213 (1988) 235.

[6] S. Catani, Yu. L. Dokshitzer and B. R. Webber, Phys. Lett. B285 (1992) 291.

[7] A. V. Anisovich et al., "Hadron Distributions in the Final State of DIS at HERA", preprint EMCSC/ELN 93-01 (1993), to appear in Nuovo Cimento.

[8] Ya. I. Azimov, Yu. L. Dokshitzer, V. A. Khoze and S. I. Troyan, Z. Phys. C27 (1985) 65.

[9] Yu. L. Dokshitzer, V. A. Khoze and S. I. Troyan, Int. Journ. Mod. Phys. A7 (1992) 1875 and Z. Phys. C55 (1992) 107.

[10] T. Sjostrand, "QCD and Jets at LEP", preprint CERN-TH.5902/90 (1990).

[11] For a detailed review, see for instance:
M. Basile et al., Nuovo Cimento 79A (1984) 1 and A. Zichichi, Proceedings of the XXIII Course of the "Ettore Majorana" Int. School of Subnuclear Physics, Erice, Italy, 1985: "Old and New Forces of Nature" (Plenum Press, New-York-London, 1988), p. 117.

[12] ZEUS Collaboration (M. Derrick et al.), "The ZEUS Detector: Status Report 1989", DESY PRC 89-01 (1989).

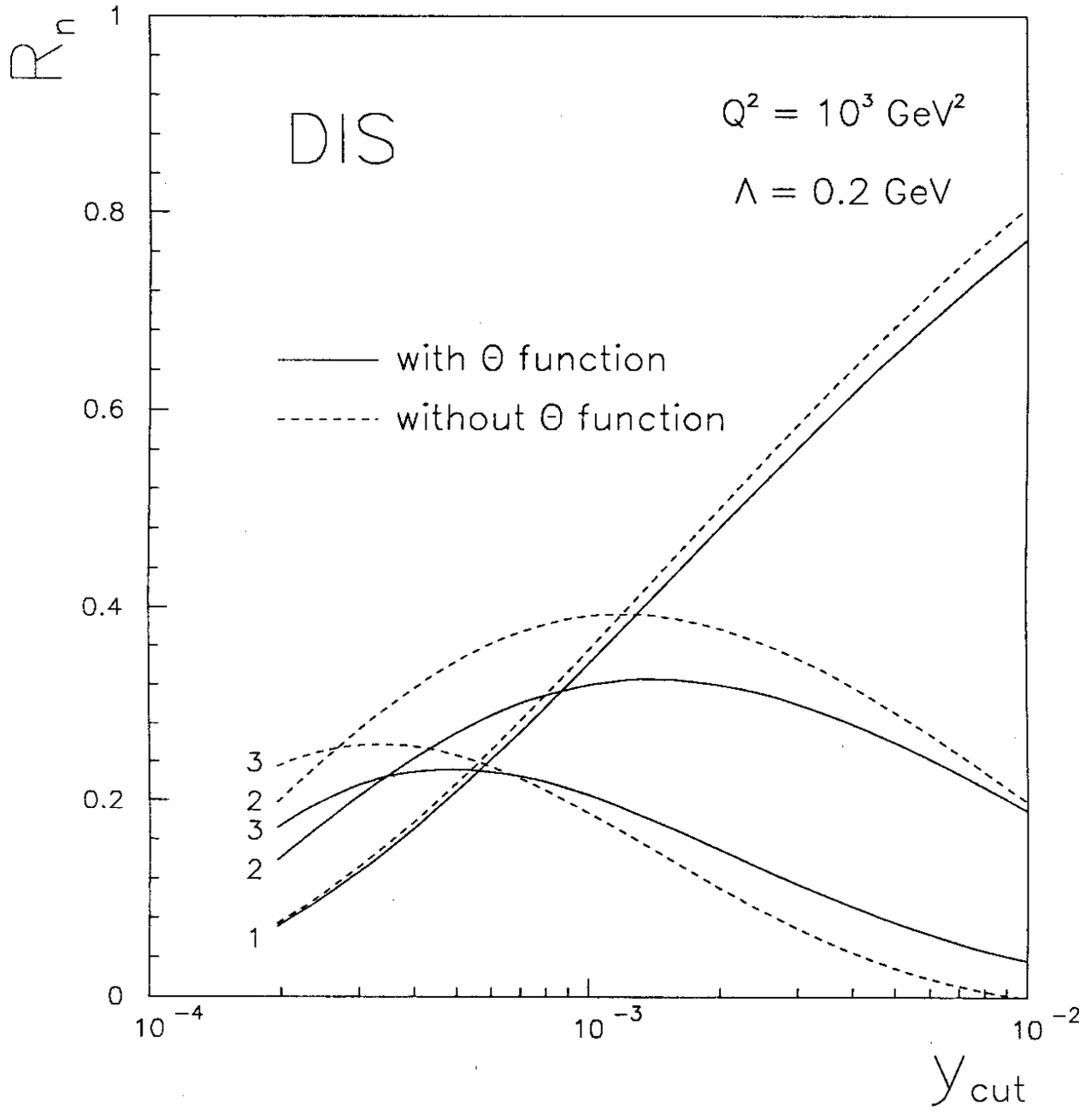
$R^C$
1
0.8
0.6
0.4
0.2
0
DIS
$Q^2 = 10^3$ GeV$^2$
$\Lambda = 0.2$ GeV
with Θ function
without Θ function
3
2
3
2
1
$10^{-4}$
$10^{-3}$
$10^{-2}$
$y_{cut}$

Fig. 1

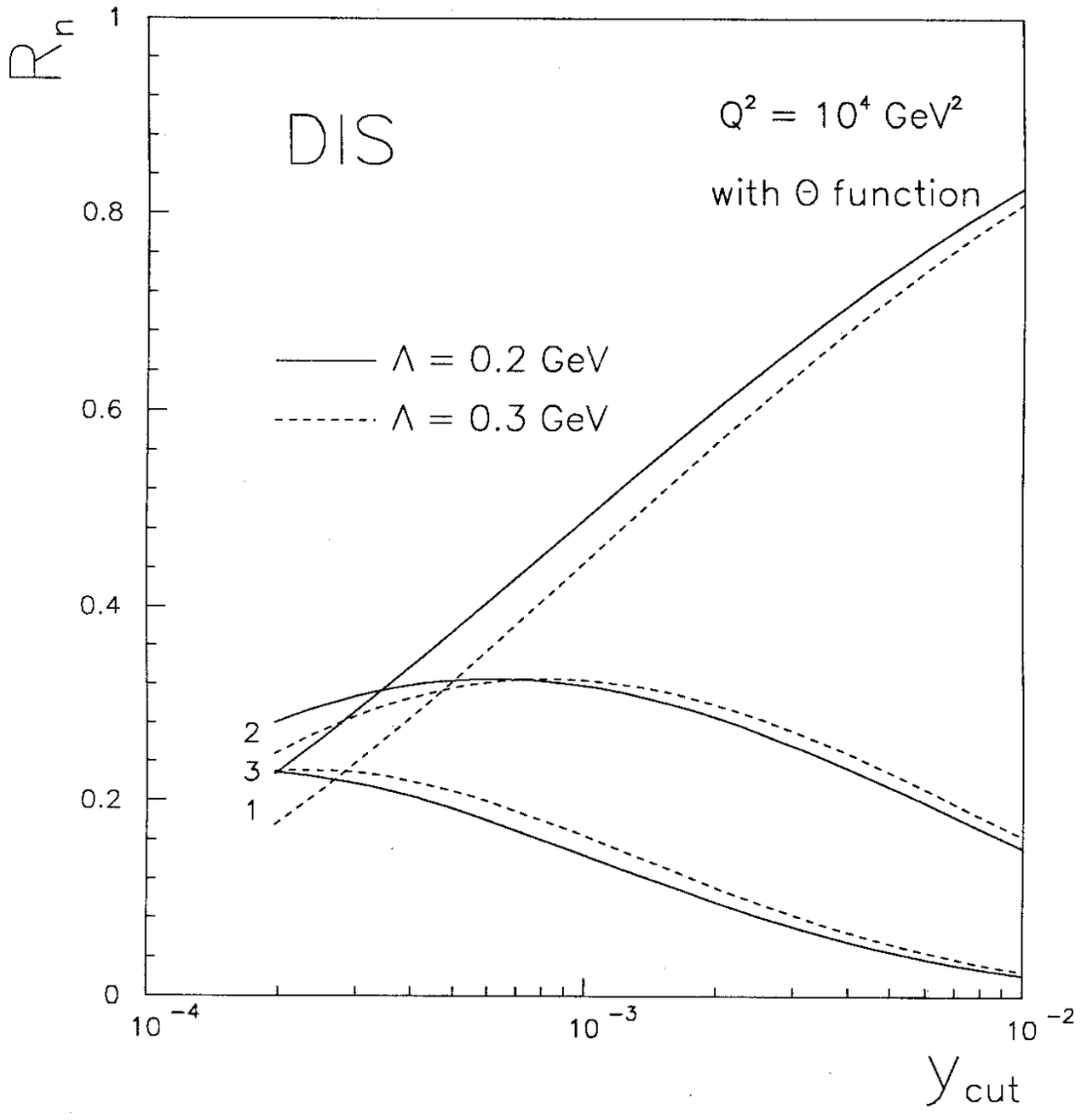
$R_n$
1
0.8
0.6
0.4
0.2
0
DIS
$Q^2 = 10^4$ GeV$^2$
with Θ function
$\Lambda = 0.2$ GeV
$\Lambda = 0.3$ GeV
2
3
1
$10^{-4}$
$10^{-3}$
$10^{-2}$
$y_{cut}$

Fig. 2

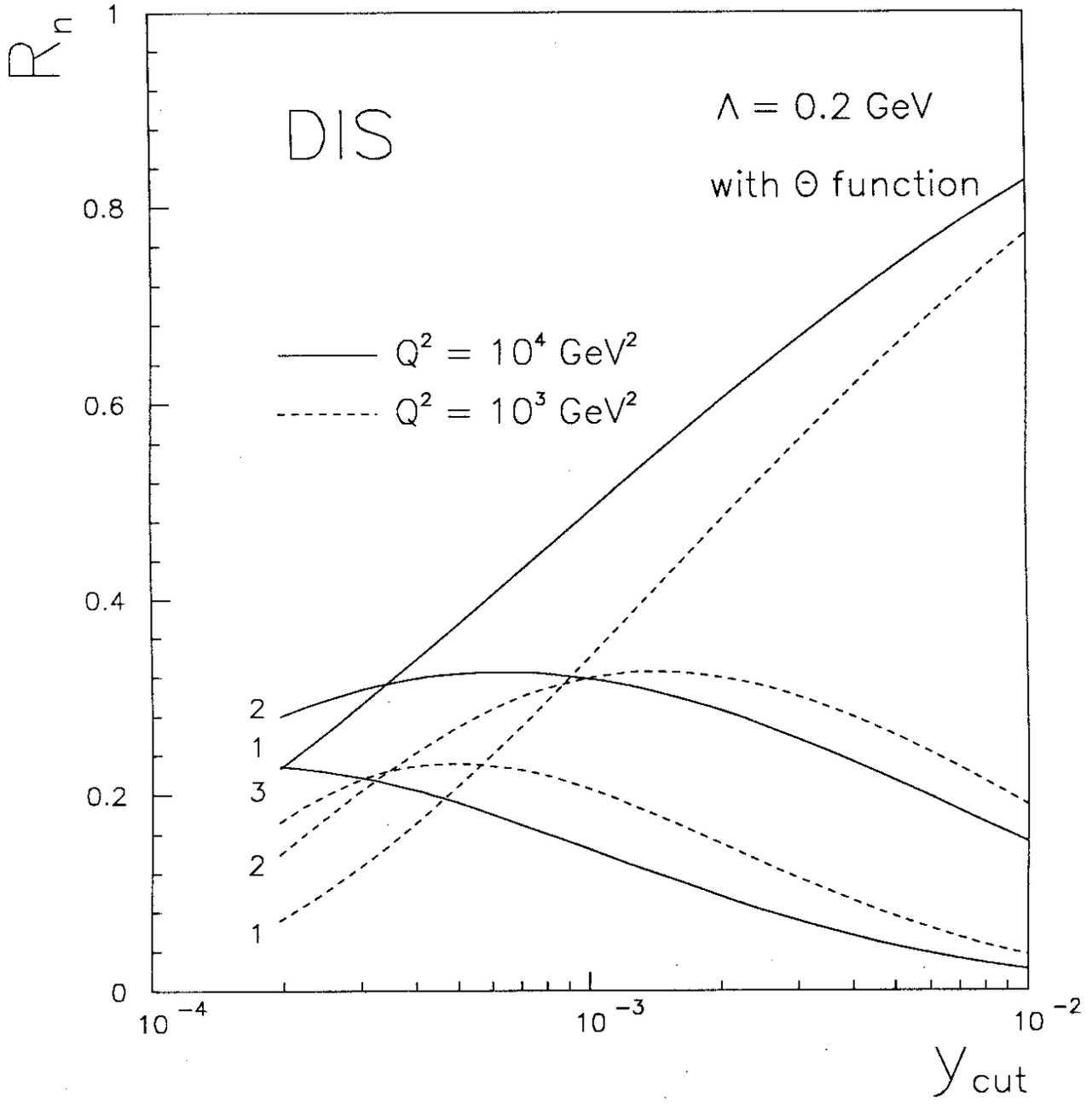
$R_n$
1
0.8
0.6
0.4
0.2
0
DIS
$\Lambda = 0.2$ GeV
with $\Theta$ function
$Q^2 = 10^4$ GeV$^2$
$Q^2 = 10^3$ GeV$^2$
2
1
3
2
1
$10^{-4}$
$10^{-3}$
$10^{-2}$
$y_{cut}$

Fig. 3

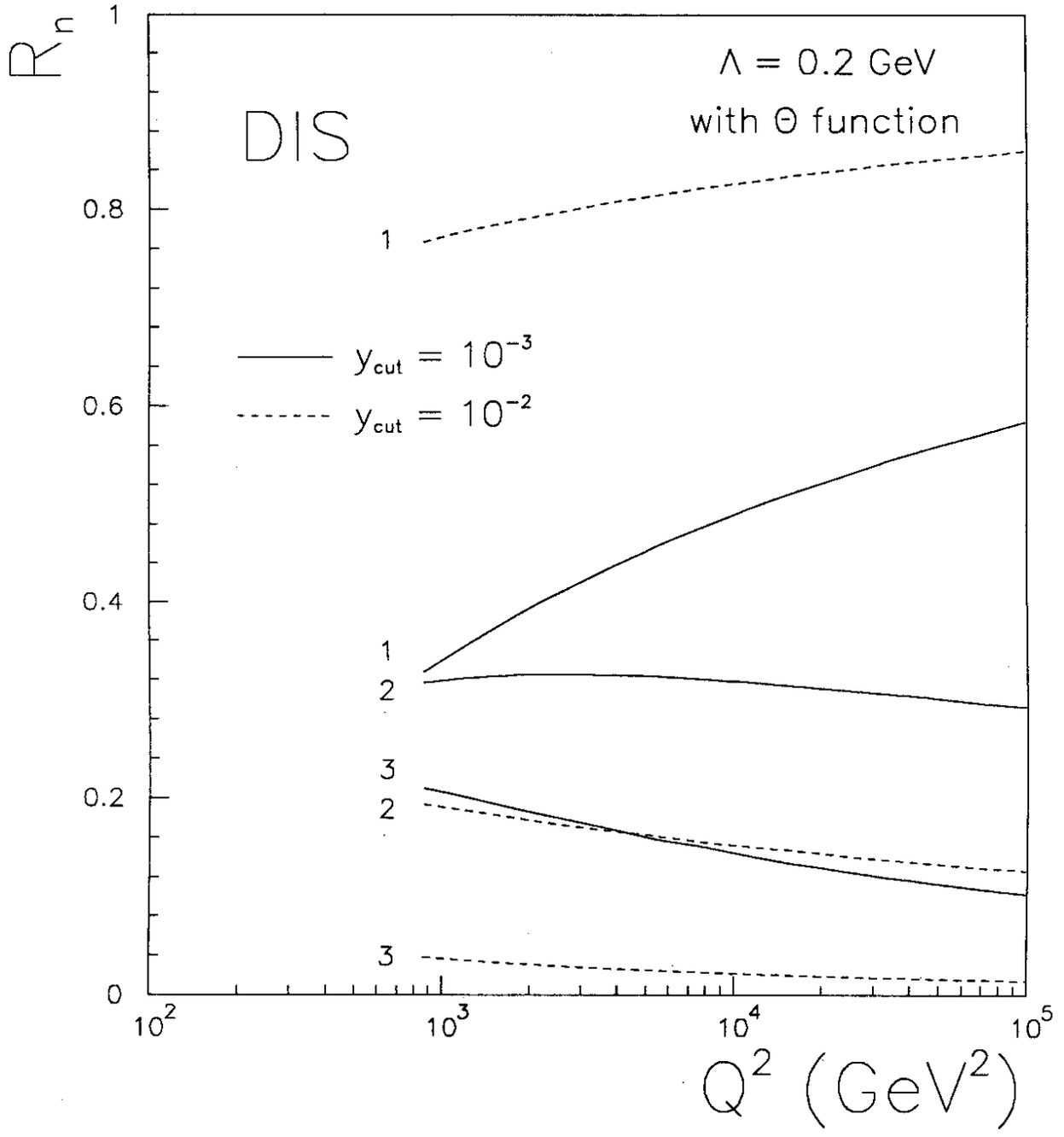
$R_n$
1
0.8
0.6
0.4
0.2
0
DIS
$\Lambda = 0.2$ GeV
with $\Theta$ function
1
$y_{cut} = 10^{-3}$
$y_{cut} = 10^{-2}$
1
2
3
2
3
$10^2$
$10^3$
$10^4$
$10^5$
$Q^2$ (GeV$^2$)

Fig. 4

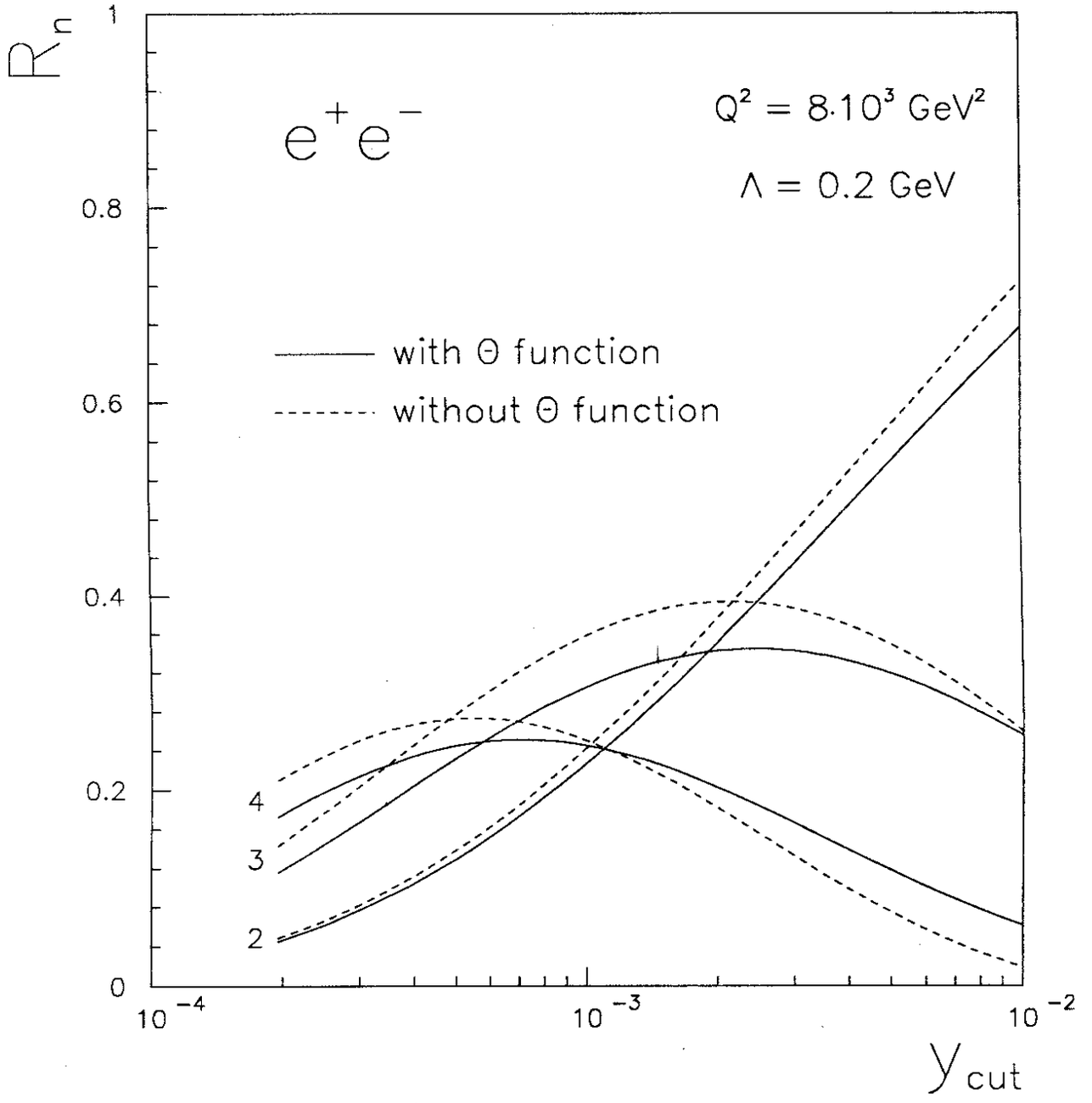
$R_n$
1
0.8
0.6
0.4
0.2
0
$e^+e^-$
$Q^2 = 8{\cdot}10^3$ GeV$^2$
$\Lambda = 0.2$ GeV
with Θ function
without Θ function
4
3
2
$10^{-4}$
$10^{-3}$
$10^{-2}$
$y_{cut}$

Fig. 5

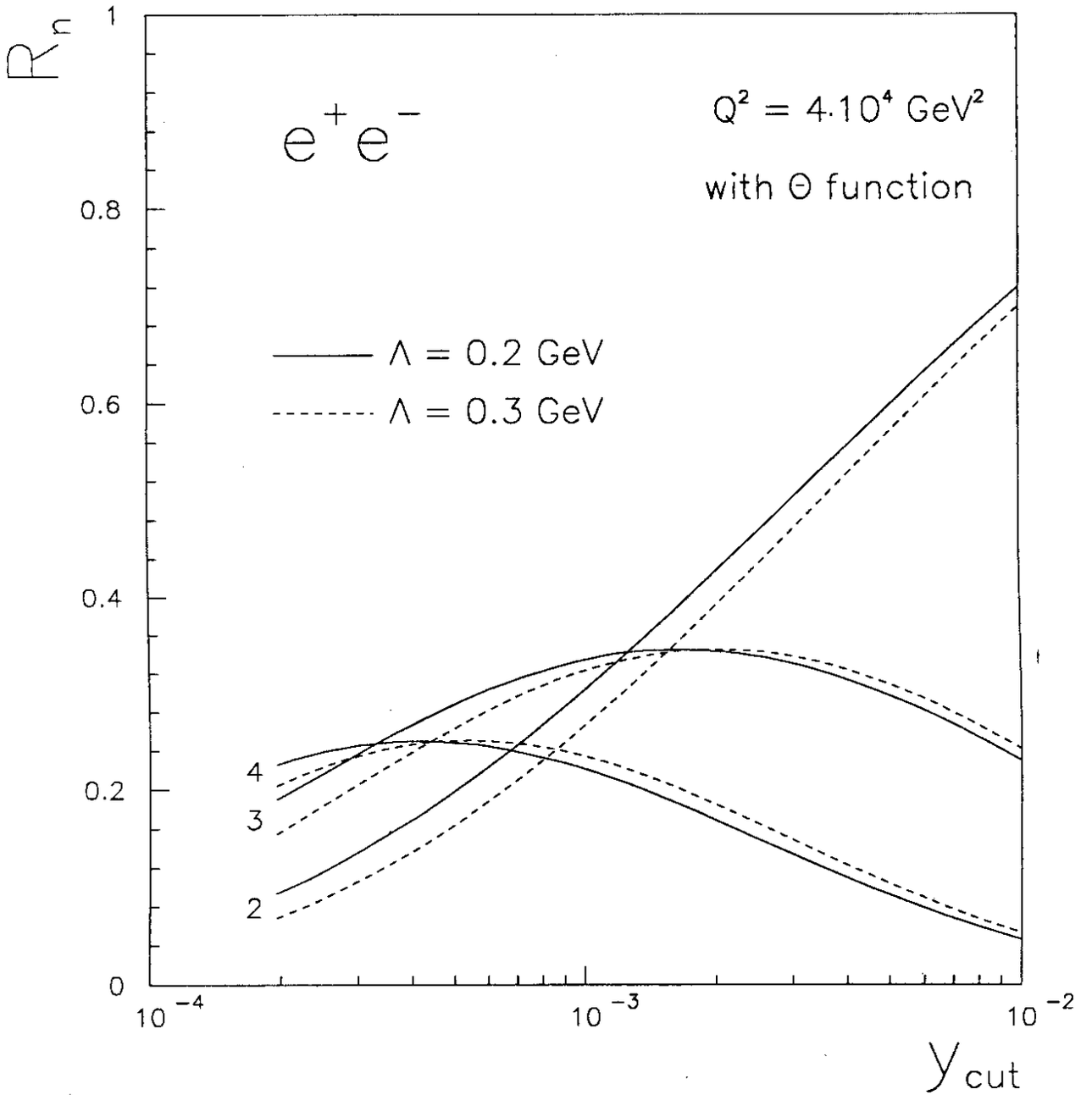
$R_n$
1
0.8
0.6
0.4
0.2
0
$e^+e^-$
$Q^2 = 4.10^4$ GeV$^2$
with Θ function
$\Lambda = 0.2$ GeV
$\Lambda = 0.3$ GeV
4
3
2
$10^{-4}$
$10^{-3}$
$10^{-2}$
$y_{cut}$

Fig. 6

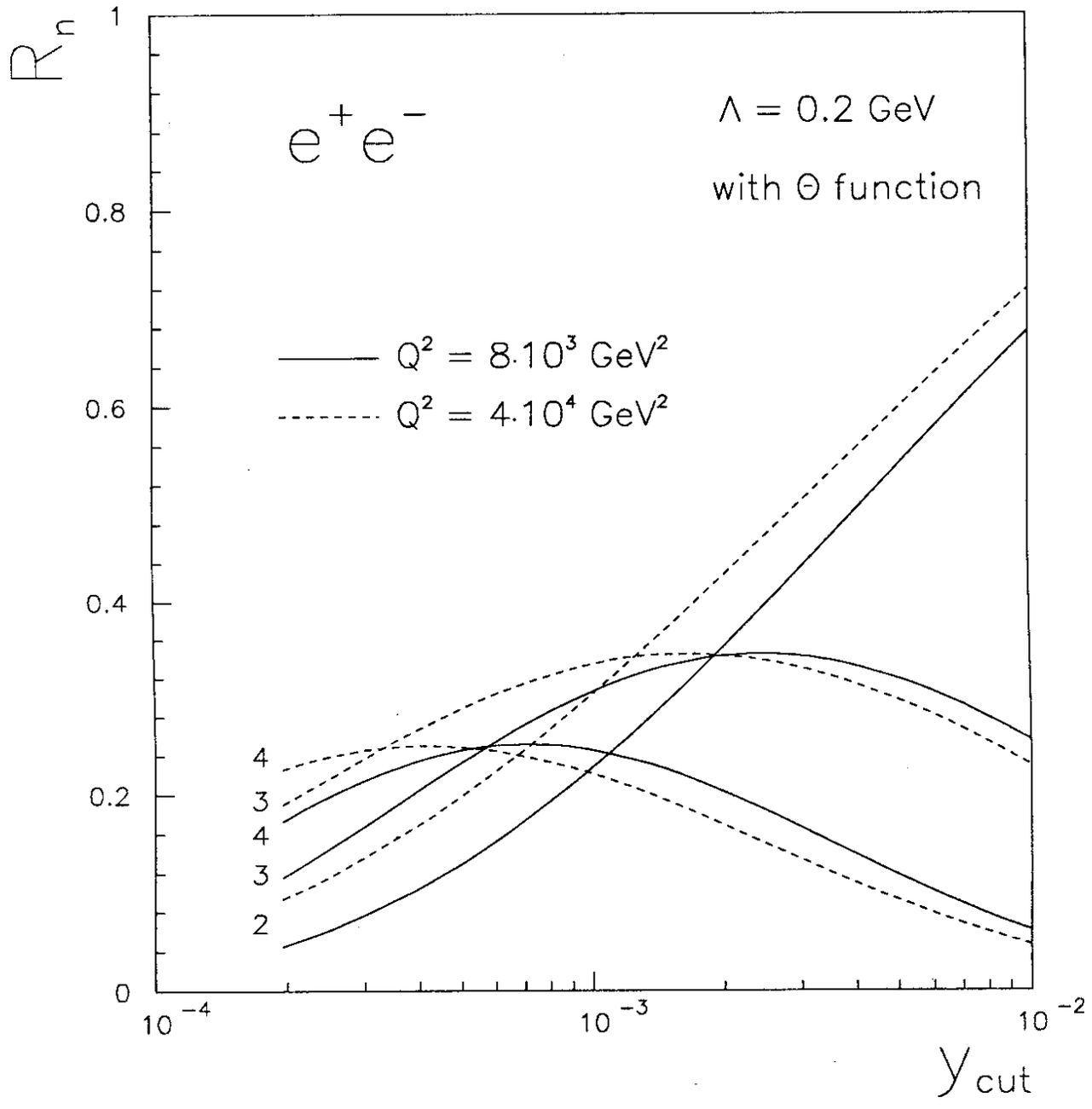
$R_n$
1
0.8
0.6
0.4
0.2
0
$e^+e^-$
$\Lambda = 0.2$ GeV
with $\Theta$ function
$Q^2 = 8.10^3$ GeV$^2$
$Q^2 = 4.10^4$ GeV$^2$
4
3
4
3
2
$10^{-4}$
$10^{-3}$
$10^{-2}$
$y_{cut}$

Fig. 7

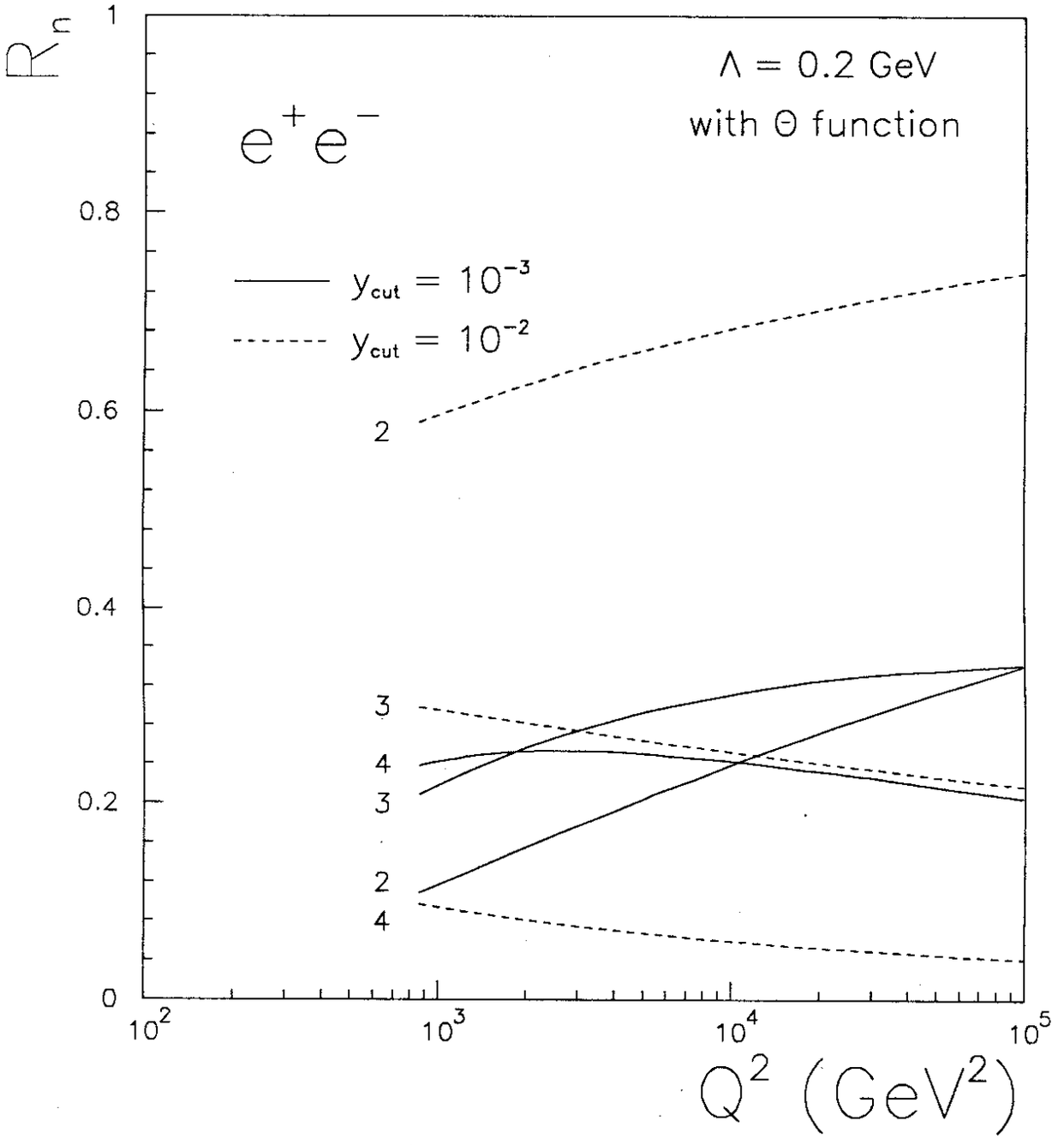
$R_n$
1
0.8
0.6
0.4
0.2
0
$e^+e^-$
$\Lambda = 0.2$ GeV
with Θ function
$y_{cut} = 10^{-3}$
$y_{cut} = 10^{-2}$
2
3
4
3
2
4
$10^2$
$10^3$
$10^4$
$10^5$
$Q^2$ (GeV$^2$)

Fig. 8

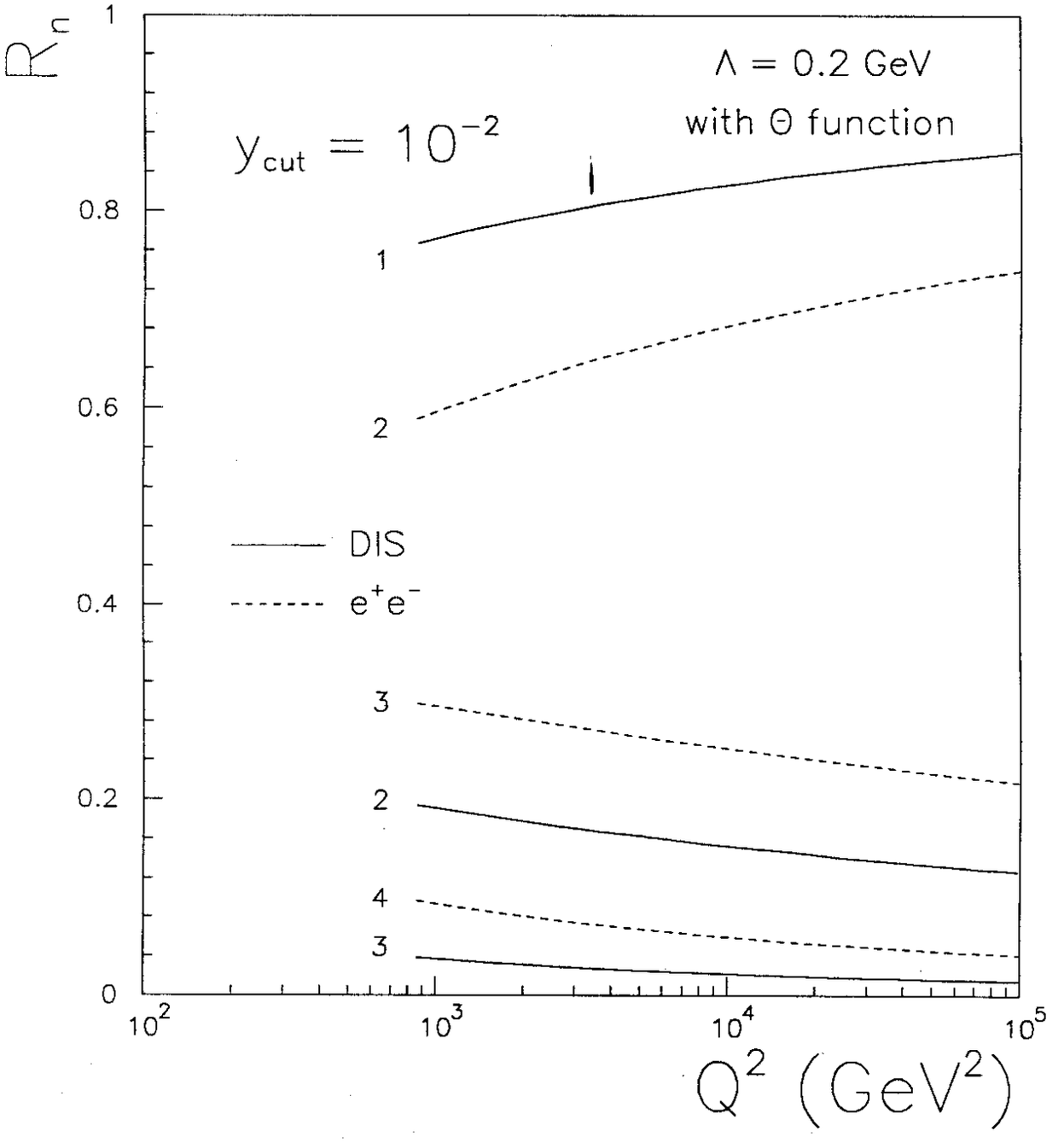
$R_n$
1
0.8
0.6
0.4
0.2
0
$\Lambda = 0.2$ GeV
with Θ function
$y_{cut} = 10^{-2}$
1
2
DIS
$e^+e^-$
3
2
4
3
$10^2$
$10^3$
$10^4$
$10^5$
$Q^2$ (GeV$^2$)

Fig. 9

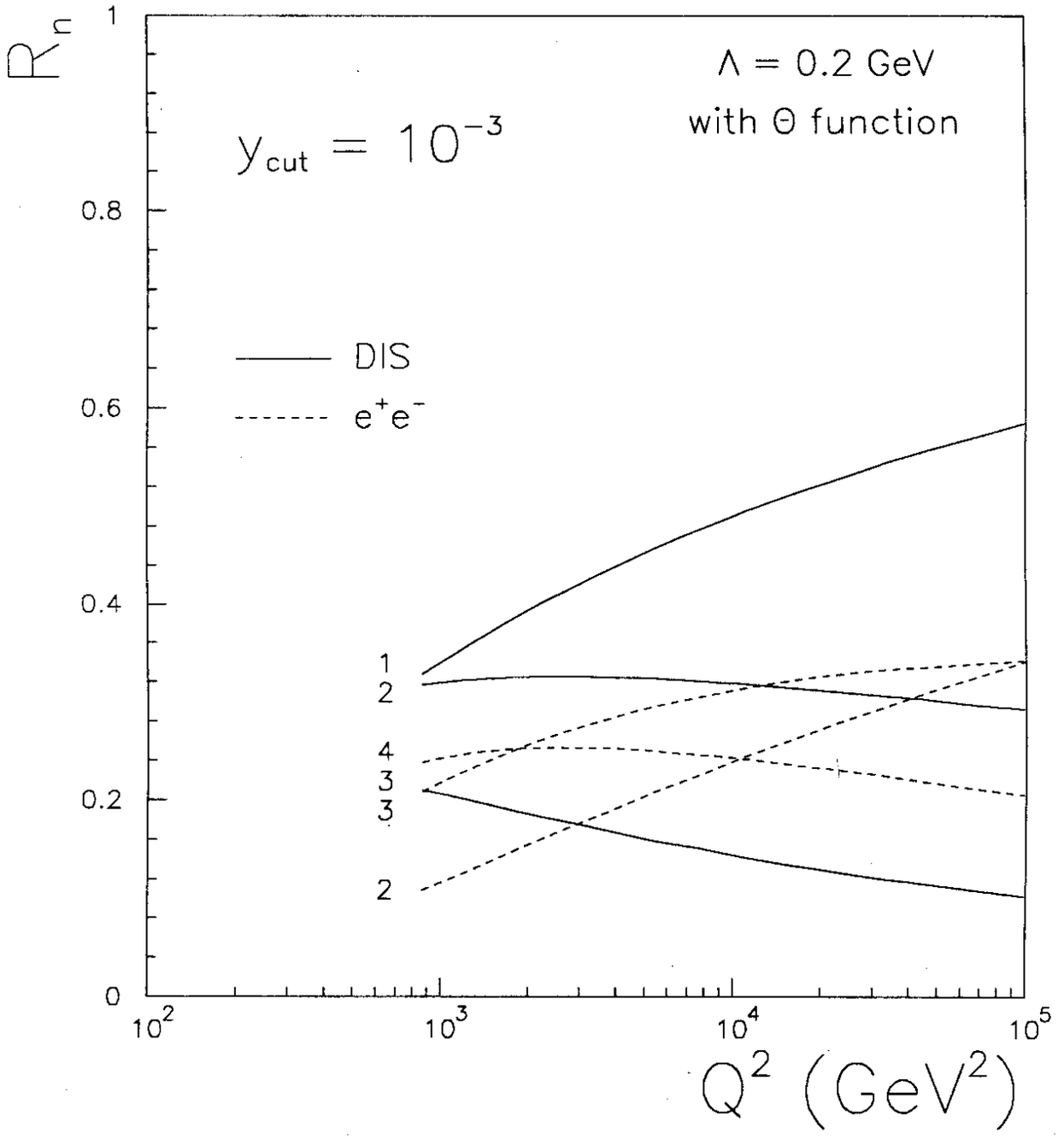
$R_c$
1
0.8
0.6
0.4
0.2
0
$\Lambda = 0.2$ GeV
with Θ function
$y_{cut} = 10^{-3}$
DIS
$e^+e^-$
1
2
4
3
3
2
$10^2$
$10^3$
$10^4$
$10^5$
$Q^2$ (GeV$^2$)

Fig. 10